

71
GPO PRICE \$ _____

CFSTI PRICE(S) \$ _____

Hard copy (HC) 5

Microfiche (MF) _____

ff 653 July 65

INFORMATION NOT TO BE
RELEASED OUTSIDE NASA
UNTIL PAPER PRESENTED

DAMPERS TO SUPPRESS WIND-INDUCED OSCILLATIONS
OF TALL FLEXIBLE STRUCTURES


By Wilmer H. Reed III and Rodney L. Duncan

NASA Langley Research Center
Langley Station, Hampton, Va.

Presented at the 10th Midwestern Mechanics Conference

FACILITY FORM 602	N 68-26832	
	(ACCESSION NUMBER)	(THRU)
	26 (PAGES)	1 (CODE)
	NASA-TMX-60432 (NASA CR OR TMX OR AD NUMBER)	32 (CATEGORY)

Fort Collins, Colorado
August 21-23, 1967



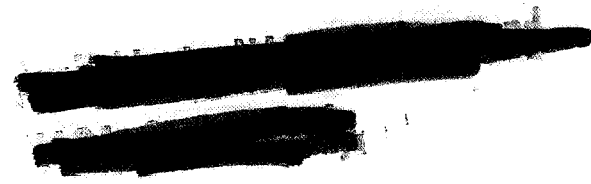
DAMPERS TO SUPPRESS WIND-INDUCED OSCILLATIONS
OF TALL FLEXIBLE STRUCTURES

By Wilmer H. Reed III and Rodney L. Duncan

NASA Langley Research Center

ABSTRACT

The paper focuses on the use of dampers to suppress wind-induced oscillations of tall, flexible structures such as stacks, antennas, and erected launch vehicles. On the basis of wind-tunnel studies with an aeroelastic model of the Saturn V launch vehicle, viscous dampers were installed on the full-scale structure to assure against excessive ground-wind-induced oscillations. Also described is a simple but effective damper recently developed to alleviate wind-induced oscillations on a U.S. Navy antenna system. This damper, which consists of chains hanging in containers, is a form of impact damper and appears to have many potential applications. Finally, the paper presents a progress report on a generalized research investigation of hanging-chain dampers.



DAMPERS TO SUPPRESS WIND-INDUCED OSCILLATIONS
OF TALL FLEXIBLE STRUCTURES

By Wilmer H. Reed III* and Rodney L. Duncan**

NASA Langley Research Center
Mail Stop 340
Telephone AC 703-722-7961, Ext. 2661
Langley Station, Hampton, Virginia 23365

INTRODUCTION

Tall, bluff-body structures such as stacks, towers, or erected launch vehicles, when exposed to a steady wind, experience not only steady but also oscillatory loads. These oscillatory loads, which act primarily in the cross-stream direction, are produced as a result of vortices that are shed from the sides of the structure. For lightly damped structures the inertia loads due to wind-excited oscillations are often considerably higher than the steady loads.

Wind-induced response of structures may be alleviated in various ways. One approach, which in practice is usually difficult to apply, requires that the structure be so designed that its significant natural frequencies do not coincide with the vortex shedding frequencies that occur in the wind speed range of interest. A second approach involves disrupting the excitation force by an aerodynamic means, such as the helical strakes developed by Scruton (ref. 1) for circular stacks. A third approach utilizes external damping devices on the structure to prevent the buildup of excessive wind-induced oscillations. This latter approach will be the subject of the present paper.

*Assistant Head, Aeroelasticity Branch.

**Aerospace Engineer, Aeroelasticity Branch.

The paper describes some recent NASA research programs which resulted in the development of dampers for erected structures. The particular erected structures in question are the Saturn V launch vehicle during its exposure to ground wind loads prior to launch, and cylindrical antenna elements in use by the U.S. Navy.

Because of its simplicity and damping effectiveness, the so-called hanging-chain damper developed for the Navy antenna appears to have many other potential applications. For this reason, a generalized research study of the hanging-chain damper was undertaken. The final section of the present paper contains a progress report on this research.

SYMBOLS

c_e	equivalent viscous damping of chain damper
d	total clearance gap between chain and its container
D	diameter of circular cylinder
e	coefficient of restitution
f	vortex shedding frequency
$F(t)$	excitation force
k	spring constant
m	mass of chain
m_e	effective mass of vibrating chain
M	lumped mass of single-degree-of-freedom system
t	time
T	integration time used in impedance measurements
V	free-stream velocity
x	displacement of single-degree-of-freedom system

x_{st} static displacement, F_0/k
 $Z_D(\omega), Z_S(\omega)$ mechanical impedance of damper and structure, respectively
 ζ viscous damping ratio
 μ ratio of chain mass to structural mass, m/M
 ω circular frequency
 ω_1 resonant frequency of system with damper attached
 ω_n undamped natural frequency, $\sqrt{k/M}$
 Subscript:
 o vector amplitude

VORTEX SHEDDING LOADS ON CIRCULAR CYLINDERS

Before discussing methods of damping wind-induced response of structures, let us first briefly consider the aerodynamic forces that produce such response. Unfortunately these forces, which originate from unsteady separated flow about bluff bodies, are not clearly understood - even on such basic shapes as a two-dimensional circular cylinder.

For example, only in recent years have definitive experiments shown that the well-known periodic nature of vortex shedding at subcritical Reynolds numbers again becomes evident at higher Reynolds numbers. These characteristics were first observed from wake measurements by Roshko (ref. 2) and more recently from force measurements on a large two-dimensional cylinder in the Langley transonic dynamics tunnel, some preliminary results of which are reported in reference 3.

Figure 1 shows the variation of vortex shedding frequency (Strouhal number) with Reynolds number for a stationary circular cylinder. The sample time histories indicate schematically the nature of the unsteady aerodynamic forces

on the cylinder. Of particular interest is the high Reynolds number range corresponding to ground wind exposure conditions for the Saturn V launch vehicle. The wind speed for Reynolds numbers based on the 33-foot lower stage diameter of the Saturn V is also shown in figure 1. Note that at a Reynolds number of about 3.5 million, corresponding to a wind speed of 10 knots for the Saturn V, the aerodynamic force begins to show definite periodic characteristics. Thus, at a wind speed where the frequency of periodic vortex shedding coincides with a natural vibration frequency of the structure, large-amplitude oscillatory response can be expected.

GROUND-WIND-LOAD STUDIES ON SATURN V

Wind-Tunnel Model Studies

Wind-tunnel studies on an aeroelastically scaled model of the Saturn V Apollo launch vehicle have indicated a potential ground-wind-loads problem. The nature of this problem is illustrated in figure 2. This figure shows that for vehicle damping of 1-percent critical ($\zeta = 0.01$), at a wind speed of about 55 knots, the dynamic response peaks up very sharply and even exceeds the design moment on the vehicle. When the structural damping is increased to $\zeta = 0.02$ the response is reduced to a level well within allowable load limits. A further description of these tests and the damping devices used to simulate structural damping in the model may be found in references 4 and 5.

On the basis of wind-tunnel data such as shown in figure 2, Marshall Space Flight Center designed and installed a damper on the Saturn facility checkout vehicle prior to its rollout in May 1966. Figure 3 is a schematic drawing of the damper system employed on the full-scale vehicle. Note that it is installed at the top of the second stage and connects between the umbilical tower and the

vehicle. The plan view shows three viscous dampers attached to the vehicle so as to damp motion in both horizontal directions. These dampers raised vehicle damping in the fundamental mode from 1.5 percent to 4.5 percent of critical damping. Although the vehicle with dampers has experienced winds up to 60 knots, its dynamic response was quite low.

NAVY ANTENNA

The damper application to be discussed next was developed by NASA Langley to suppress wind-excited oscillations observed on a Navy antenna system (see ref. 6). The system consists of an array of antennas and reflectors erected on the ground to form a pattern of concentric circles. An aerial photograph of a typical antenna site is shown in figure 4. The structural elements of interest for the present purpose are the high band antennas, 120 of which are equally spaced on the 1000-foot-diameter outer circumference of the array (see closeup view in fig. 4). These 24-foot tall cantilevered structures have a 16-inch-diameter circular base on which is mounted a 6-inch-diameter aluminum mast.

Wind-induced bending oscillations of the masts have been observed over a range of wind speeds including light winds. These oscillations are believed to be the primary cause of crack damage found in a conical fiber-glass insulator, which also serves as the primary load-carrying member between the mast and the base structure.

To investigate methods of suppressing these bending oscillations, wind-tunnel tests of a full-size antenna were conducted in the Langley transonic dynamics tunnel.

In considering various modifications which could be employed on antennas in the field, it was necessary to rule out those that would require guy wires

or would alter the exterior surface of the upper mast. Thus, aerodynamic spoilers, such as helical strakes, were not considered in this study.

The modification found to be the most effective in reducing the response was the damping device illustrated in figure 5. This damper is simply a cluster of hanging chains suspended inside the tip of the antenna mast. Each chain is covered with a flexible plastic tube and the entire cluster enclosed by a sheet rubber shroud.

The damper weighs 12 pounds. Its effect on the antenna, which weighs 261 pounds, is to increase damping of the fundamental mode from about 0.5 percent to 10 percent of critical damping - a twentyfold increment.

The effect of the damper on antenna dynamic response due to vortex shedding loads is readily apparent from figure 6. The figure shows the maximum dynamic bending moment, which was measured at the base of the upper mast during a 2-minute data sampling period, is plotted as a function of wind speed. Also shown on the right side of the figure are the free-vibration time histories from which the zero-wind-speed damping was determined.

Of particular interest is the sharply defined peak response occurring at 5 knots on the undamped system. At this velocity the response was essentially a pure sinusoidal motion in the cross-stream direction. The frequency was that of the antenna fundamental cantilever mode and the corresponding tip motion was ± 0.6 inch (0.1 mast diameter). This peak is indicative of coincidence between the vortex shedding frequency and a natural frequency of the antenna. At higher wind speeds the antenna response is also predominantly at the fundamental frequency, but the amplitude of motion tends to build up and die down randomly. Also, as the wind speed increased the response in the streamwise direction became almost as large as that in the cross-stream directions.

With the damper installed there was no indication of the response peak at 5 knots and the response at all other speeds was significantly reduced. In fact, it is interesting to note that with the damper installed the response at wind speeds up to 60 knots is below the response peak at 5 knots for the unmodified antenna.

FURTHER CHAIN DAMPER RESEARCH

General Remarks

To further evaluate the characteristics of chain dampers and identify important parameters, some generalized experimental studies were recently initiated at Langley Research Center. This section of the paper will briefly describe these studies and present some of the initial results.

A chain damper is considered to be in a category of dampers which operate on the principle that energy is dissipated when one mass impacts against another. In the literature, such dampers are generally referred to as impact dampers or acceleration dampers. Some basic studies of impact dampers are reported in references 7, 8, and 9. These studies treat an idealized model consisting of a frictionless mass which is free to oscillate in a gap between the walls of a container attached to a single-degree-of-freedom (mass-spring) structure. The forced response of the combined system is analyzed as a function of such parameters as the ratio of damper mass to structure mass, the clearance gap distance relative to the vibration amplitude, and the coefficient of restitution between the damper mass and its container. In order to interpret the performance characteristics of chain dampers in terms of what is known from these previous basic studies, it was decided to investigate on a single chain rather than a chain cluster such as was utilized in the Navy antenna. The chain

damper configuration chosen for study consists of a chain that hangs in a vertical channel of rectangular cross section. The variables of primary interest are: the total clearance gap between the chain and the container walls in the direction of motion, the vibration amplitude of the container, and the length and mass of chain.

Mechanical Impedance Measurements

The mechanical impedance of a damper may be defined as

$$Z_D(\omega) = \left(\frac{F_O}{\dot{x}_O} \right)_{\text{damper}} \quad (1)$$

where F_O is the amplitude of sinusoidal force acting at the damper mount point required to oscillate the mount point at a velocity $\dot{x}_O e^{i\omega t}$. The real and imaginary parts of $Z_D(\omega)$ signify force components in phase and 90° out of phase with the velocity. If the impedance of the damper and the impedance of the structure at the damper attachment point are known, the dynamic characteristics of the combined system can be readily obtained.

Consider a damper to be attached to a single-degree-of-freedom structure having a mass M and a spring constant k . The external force $F(t)$ on the system is balanced by inertia and spring forces of the structure plus damper forces. The damper forces will be assumed to have the form of a reactance force $m_e \ddot{x}$ and an equivalent viscous damping force $c_e \dot{x}$.

$$F(t) = (M\ddot{x} + kx)_{\text{structure}} + (m_e \ddot{x} + c_e \dot{x})_{\text{damper}} \quad (2)$$

The damper coefficients m_e and c_e are to be determined experimentally and will in general depend on both the frequency and the amplitude of vibration. The term m_e may be either positive or negative - positive when the reactance force acts as an equivalent mass and negative when it acts as an equivalent

spring. The complete dynamic system can be represented as separate mechanical impedances connected in parallel; that is,

$$F_O = [Z_S(\omega) + Z_D(\omega)] \dot{x}_O \quad (3)$$

Substitution of $x = x_O e^{i\omega t}$ and $F = F_O e^{i\omega t}$ into equation (2) gives the following expressions for structure and damper impedances:

$$Z_S(\omega) = i\left(\omega M - \frac{k}{\omega}\right) \quad (4a)$$

$$Z_D(\omega) = c_e + i\omega m_e \quad (4b)$$

Also from equation (2), the forced response in terms of displacement can be written

$$\frac{F_O}{x_O} = \left(-\omega^2 M - \omega^2 m_e + k\right) + i(c_e \omega) \quad (5)$$

A somewhat more convenient nondimensional form of equation (5) is (see symbol list for notation)

$$\frac{x_{st}}{x_O} = \left[1 - \left(\frac{\omega}{\omega_n}\right)^2 \left(1 + \mu \frac{m_e}{m}\right)\right] + i \left[\mu \left(\frac{\omega}{\omega_n}\right)^2 \frac{c_e}{m\omega}\right] \quad (6)$$

The nondimensional damper parameters in equation (6) to be determined by experiment are m_e/m and $c_e/m\omega$. Figure 7 illustrates the technique by which these parameters are measured. The damper is mounted on a light platform which is constrained to move horizontally. The platform is oscillated sinusoidally by means of an electric variable-speed motor. The driving force $F(t)$ is measured by a strain-gage load cell. This force signal is amplified and fed to a sin-cos potentiometer which is mechanically connected to and rotates with the crank-arm drive shaft. Thus, the two potentiometer outputs are voltages proportional to the products $F(t) \sin \omega t$ and $F(t) \cos \omega t$. By use of analog

computer components, these products are then integrated over a large number of oscillations to obtain the force in phase and 90° out of phase with the damper motion. With $F(t)$ assumed to be of the form $m_e \ddot{x} + c_e \dot{x}$ and with $x = x_0 \sin \omega t$ it can be shown that these integrations produce

$$R(\omega) = - \int_0^T F(t) \sin \omega t \, dt = \frac{m_e x_0 \omega^2 T}{2}$$

$$I(\omega) = - \int_0^T F(t) \cos \omega t \, dt = - \frac{c_e x_0 \omega T}{2}$$

where the integration time T is assumed to be large relative to the period of oscillation. (In the present studies T was 20 seconds, whereas the period of oscillation varied from 1.5 to 0.15 seconds.) Actually, the quantities m_e and c_e are determined from the difference between the integrator outputs with and without the chain in the container. Thus, the container and platform masses are not included in m_e , and, similarly, the small residual damping in the platform support system has been removed from c_e .

Some typical experimental results showing the variations of $c_e/m\omega$ and m_e/m with frequency are presented in figure 8 for two damper configurations. One damper has a parallel-wall container with a clearance gap $d = 1.47$ inches. The other has a tapered-wall container such that the clearance gap is essentially zero at the chain suspension point and 1.47 inches (same as the parallel walls) at the free end of the chain. The chain in both dampers is 33 inches long and weighs 3.4 pounds. These chains are enclosed in cylindrical sheet-rubber sleeves which are used in place of the plastic tube covering discussed previously in figure 5. It was found that covering the chains in this way produced two favorable effects: the damping effectiveness increased and the chain-rattling noises which otherwise occur with a bare chain were essentially eliminated.

Note from the sketches on the left side of figure 8 that the parallel-wall damper has two distinct modes of chain vibration. At frequencies below 4 cps virtually the entire length of chain impacts against the container walls. Two such impacts occur during each oscillation cycle. The damping parameter $c_e/\omega n$ reaches a constant value near 2.0 which is held until the frequency exceeds about 4 cps. At this frequency both the damping and the reactance curves break sharply and the chain vibration mode shape switches form as indicated in the sketch. This break frequency is dependent on the ratio of the clearance gap to the amplitude of oscillation. For the data presented in figure 8, this ratio was $d/x_0 = 4.74$.

The tapered-wall damper has an advantage over the parallel-wall damper in that the damping is less dependent on vibration amplitude. Since in a tapered container the gap distance varies continuously along the chain length, impact damping will occur over a broader range of oscillation amplitudes. However, the advantage of tapered walls is somewhat offset by the fact that for any given amplitude only a part of the chain is operating at the best gap distance. Note, for example, in figure 8 that for tapered walls $c_e/\omega n$ approaches a maximum of 1.25 as compared with 2.0 for parallel walls.

Application of Damper Impedance Measurements

To further evaluate the damping characteristics of a hanging chain, it is instructive to interpret the impedance measurements of figure 8 in terms of the maximum forced response of a single-degree-of-freedom system with chain dampers attached.

From equation (6) the frequency of maximum response ω_1 may be determined approximately by setting the real part of the equation equal to zero and solving for ω_1/ω_n

$$\frac{\omega_1}{\omega_n} = \frac{1}{\sqrt{1 + \mu \left(\frac{m_e}{m} \right)}} \quad (7)$$

This frequency, substituted into the imaginary part of equation (6), gives the amplitude of maximum response

$$\left| \frac{x_o}{x_{st}} \right|_{\max} = \frac{1 + \mu \left(\frac{m_e}{m} \right)}{\mu \left(\frac{c_e}{m\omega} \right)} \quad (8)$$

As an approximation, assume that the damper impedance is constant over the frequency range of interest. On the basis of data in figure 8 for the parallel-wall damper let $c_e/m\omega = 2.0$ and $m_e/m = 1.0$. With these values substituted into equation (8), the maximum response in terms of the ratio of chain mass to structure mass becomes

$$\left| \frac{x}{x_{st}} \right|_{\max} = \frac{1 + \mu}{2\mu} \quad (9)$$

It is also of interest to compare the maximum response of a chain damped system with that for systems having other forms of damping. For example, the maximum response of a lightly damped structure with viscous damping is

$$\left| \frac{x}{x_{st}} \right|_{\max} = \frac{1}{2\zeta} \quad (10)$$

Thus, by equating equations (9) and (10) the equivalent viscous damping ratio is

$$\zeta_{\text{equivalent}} = \frac{\mu}{1 + \mu} \quad (11)$$

In other words, equation (11) indicates that a chain damper which weighs 5 percent of the lumped structural mass, for example, would produce the equivalent of about 4.8 percent of critical viscous damping.

Consider next the idealized impact damper analyzed in references 7 through 9. The maximum forced response of a single-degree-of-freedom system with an impact damper attached is derived in reference 9, where it is shown that for a condition of optimum gap clearance the maximum response is

$$\left| \frac{x}{x_{st}} \right|_{max} = \frac{\pi(1-e)}{4(1+e)} \frac{1+\mu}{\mu} \quad (12)$$

where e is the coefficient of restitution between the impacting masses. It is of interest to note that when $e = 0.22$ this equation becomes identical to equation (9) for a chain damper.

The ultimate aim of the experimental studies in progress at the time of this writing will be to identify and isolate the important parameters so that chain dampers may be designed efficiently for various specific applications.

CONCLUDING REMARKS

This paper attempts to demonstrate that dampers can provide an effective means of suppressing wind-induced oscillations of launch vehicles, antennas, and similar tall flexible structures. As a consequence of wind-tunnel model studies, which indicated a potentially severe ground-wind-load problem on the Saturn V vehicle, viscous dampers were installed on the full-scale structure. The paper also describes a simple and effective damper recently developed for Navy antennas but which appears to have other promising applications. Finally, a generalized research program aimed at determining chain-damper design parameters is described and some initial results in the form of mechanical impedance measurements are presented.

REFERENCES

1. Scruton, C.; and Flint, A. R.: Wind Excited Oscillations of Structures.
Paper No. 6758, Proc. Inst. Civil Engrs., vol. 27, pp. 673-702, April 1964.
2. Roshko, A.: Experiments on the Flow Past a Circular Cylinder at Very High Reynolds Number. J. Fluid Mech., vol. 10, pp. 345-356, 1961.
3. Cincotta, Joseph J.; Jones, George W., Jr.; and Walker, Robert W.: Experimental Investigation of Wind Induced Oscillation Effects on Cylinders in Two-Dimensional Flow at High Reynolds Numbers. Presented at Meeting on Ground Wind Load Problems in Relation to Launch Vehicles, NASA Langley Research Center, June 7-8, 1966.
4. Reed, Wilmer H., III: Models for Obtaining Effects of Ground Winds on Space Vehicles Erected on the Launch Pad. Conference on the Role of Simulation in Space Technology, Virginia Polytechnic Institute, Engineering Extension Series, Circular No. 4, Part C, Aug. 17-21, 1964.
5. Farmer, Moses G.; and Jones, George W., Jr.: Summary of Langley Wind Tunnel Studies of Ground-Wind Loads on Launch Vehicles. Presented at the Meeting on Ground Wind Load Problems in Relation to Launch Vehicles, NASA Langley Research Center, June 7-8, 1966.
6. Farmer, Moses G.; and Reed, Wilmer H., III: Study of Wind Excited Oscillations of High Band Wullenwebber Antenna. Langley Working Paper LWP 324, November 1966.
7. Lieber, Paul; and Jensen, D. P.: An Acceleration Damper: Development, Design, and Some Applications. A.S.M.E. Transactions, vol. 67, no. 7, Oct. 1945, pp. 523-530.

8. Arnold, R. N.: Response of an Impact Vibration Absorber to Forced Vibration.
Ninth International Congress of Applied Mechanics, Univ. of Brussels,
vol. 7, 1957, pp. 395-418.
9. Warburton, G. B.: On the Theory of the Acceleration Damper. J. Applied
Mech., vol. 24, Trans. ASME, vol. 79, 1957, pp. 322-324.

ACKNOWLEDGMENT

The authors are indebted to Mr. William G. Johnson, Jr., who, serving at Langley Research Center under the NASA/Virginia Polytechnic Institute Student Coop Program, conducted the chain-damper impedance tests reported herein.

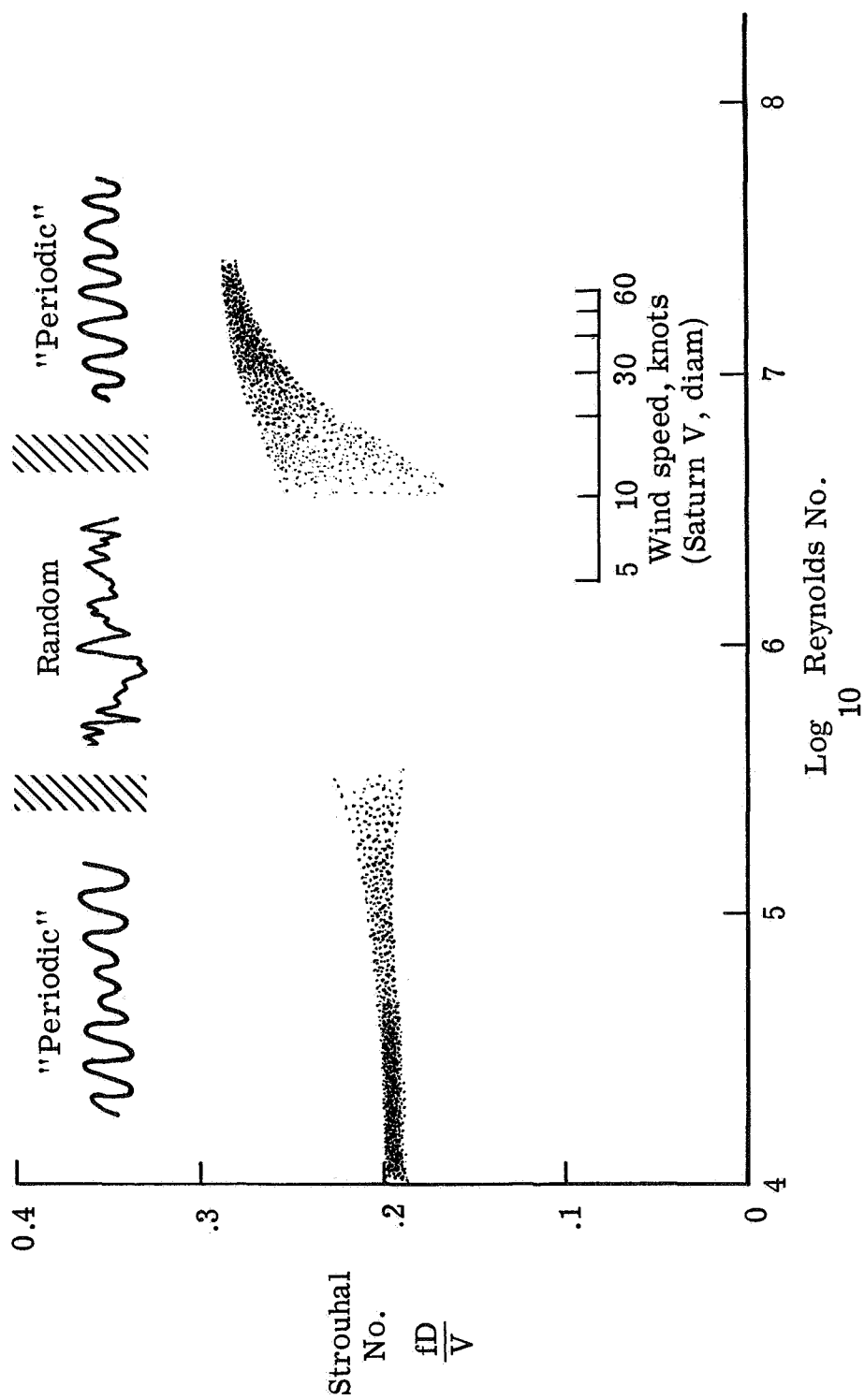


Figure 1.1.- Vortex shedding characteristics for a stationary circular cylinder.

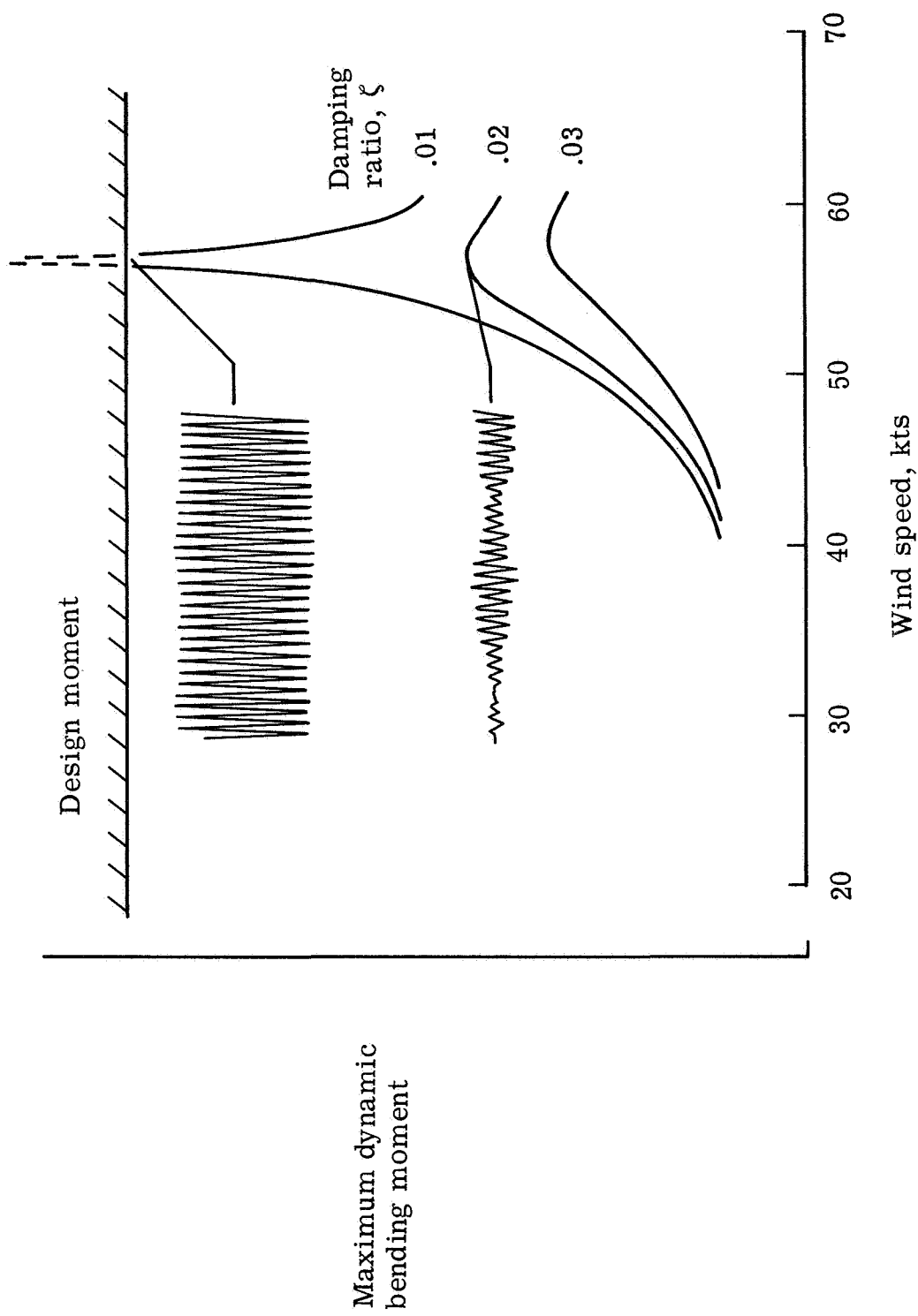


Figure 2.- Effect of damping on Saturn V ground wind loads.

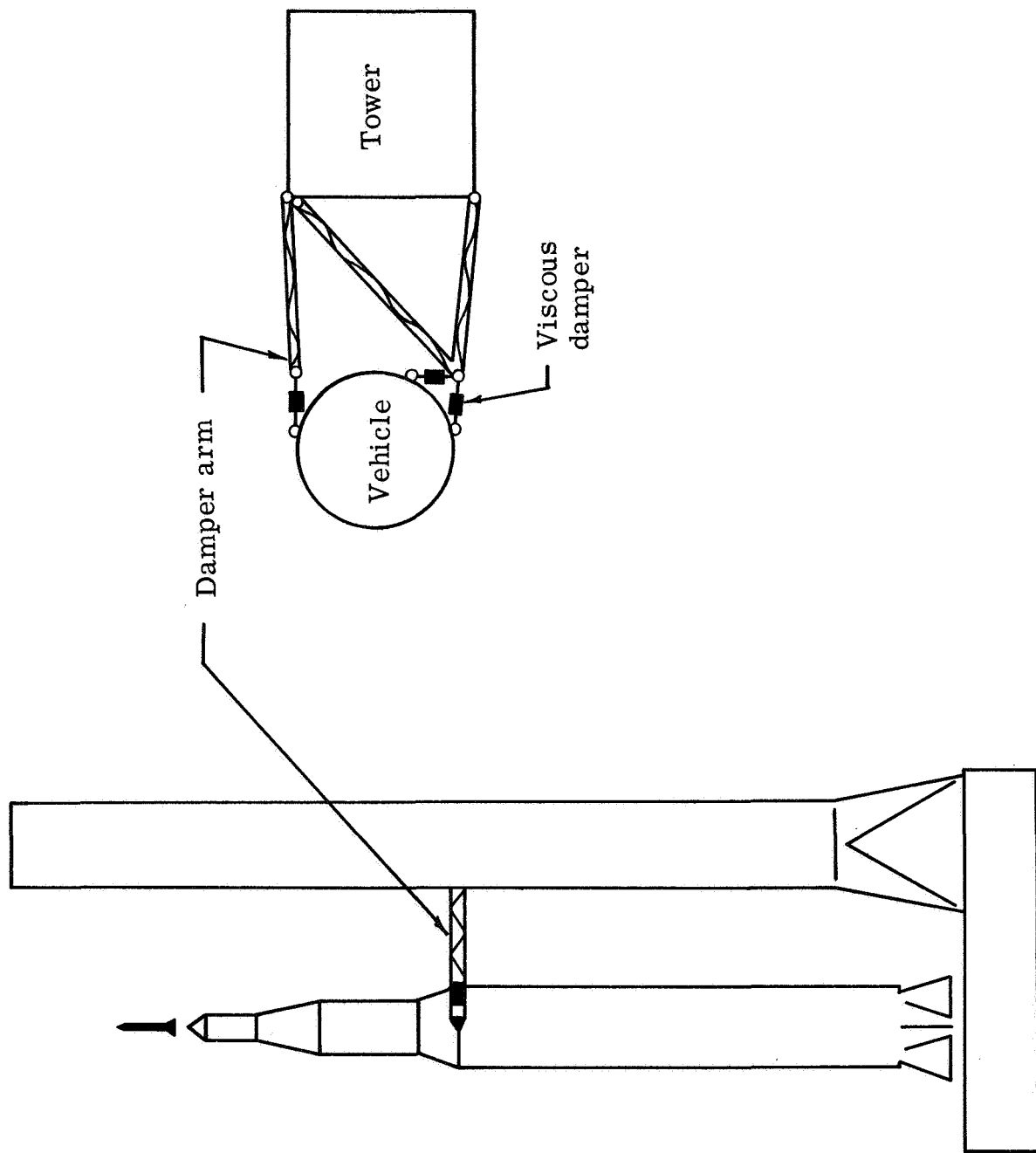


Figure 3.- Damper installation on Saturn 500-F (facility checkout vehicle).

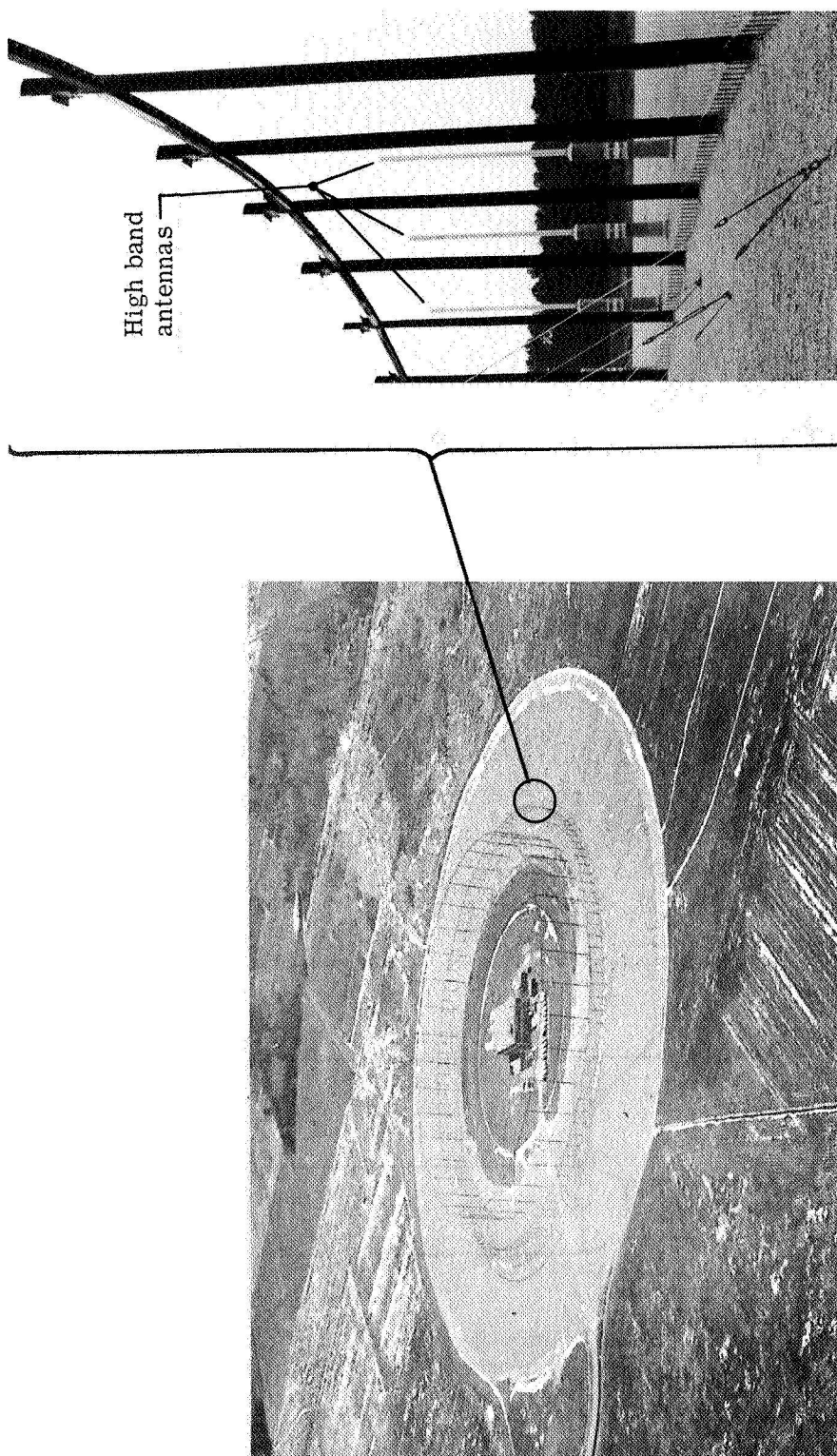


Figure 4.- Wullenweber antenna site at Northwest, Virginia.

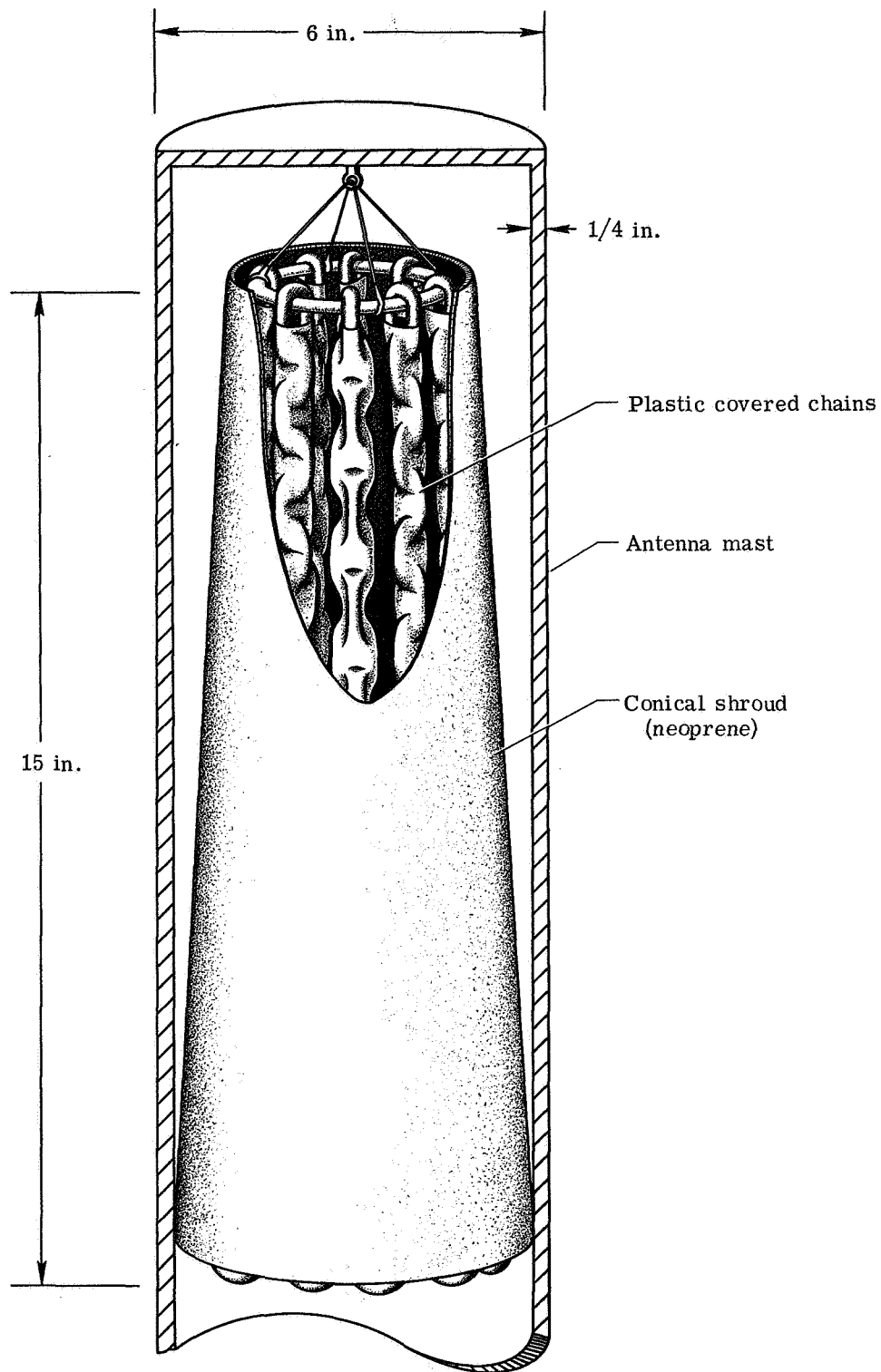


Figure 5.- Shrouded-chain damper installation in tip of antenna mast.

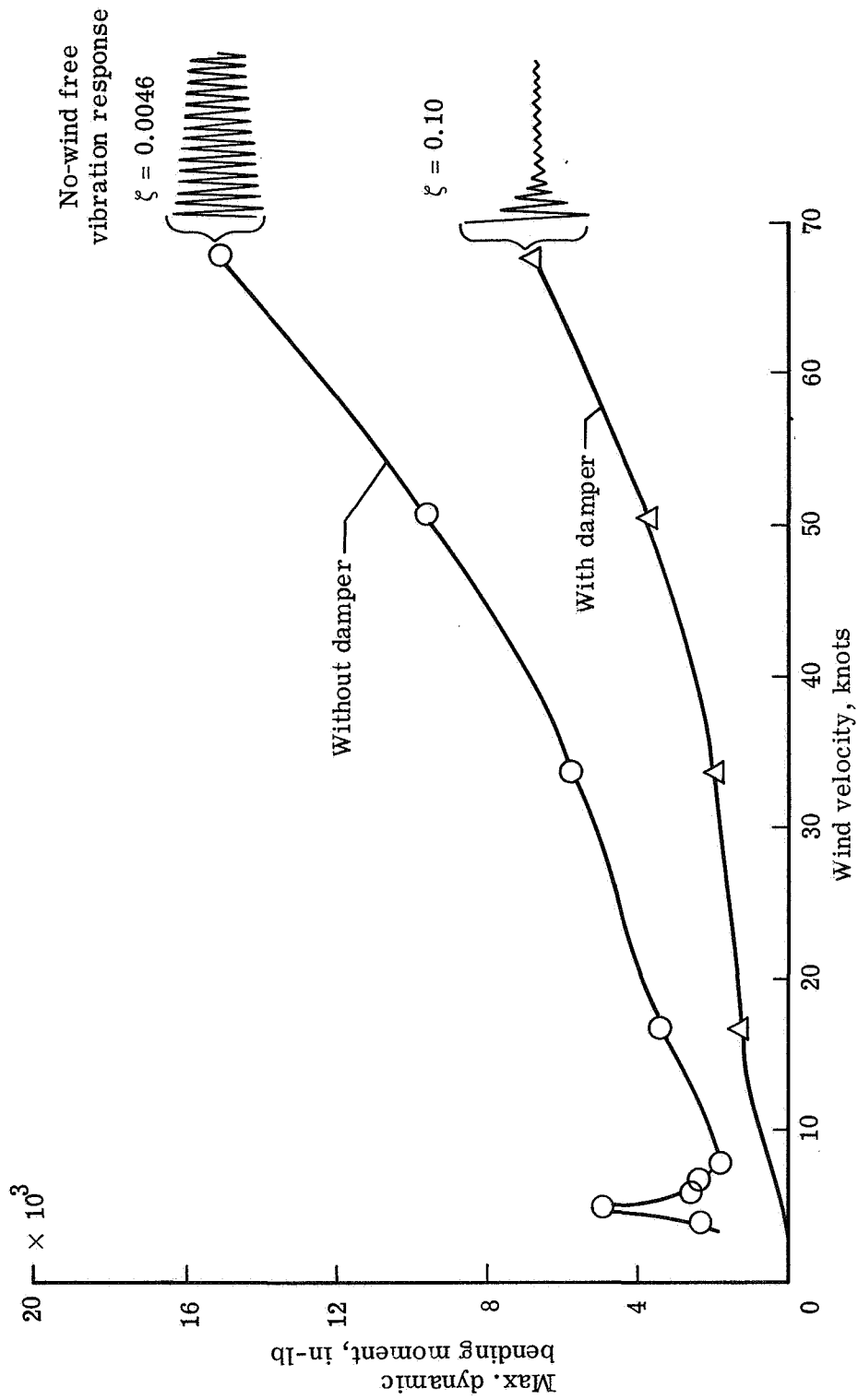


Figure 6.- Effect of chain damper on antenna wind-induced oscillations.

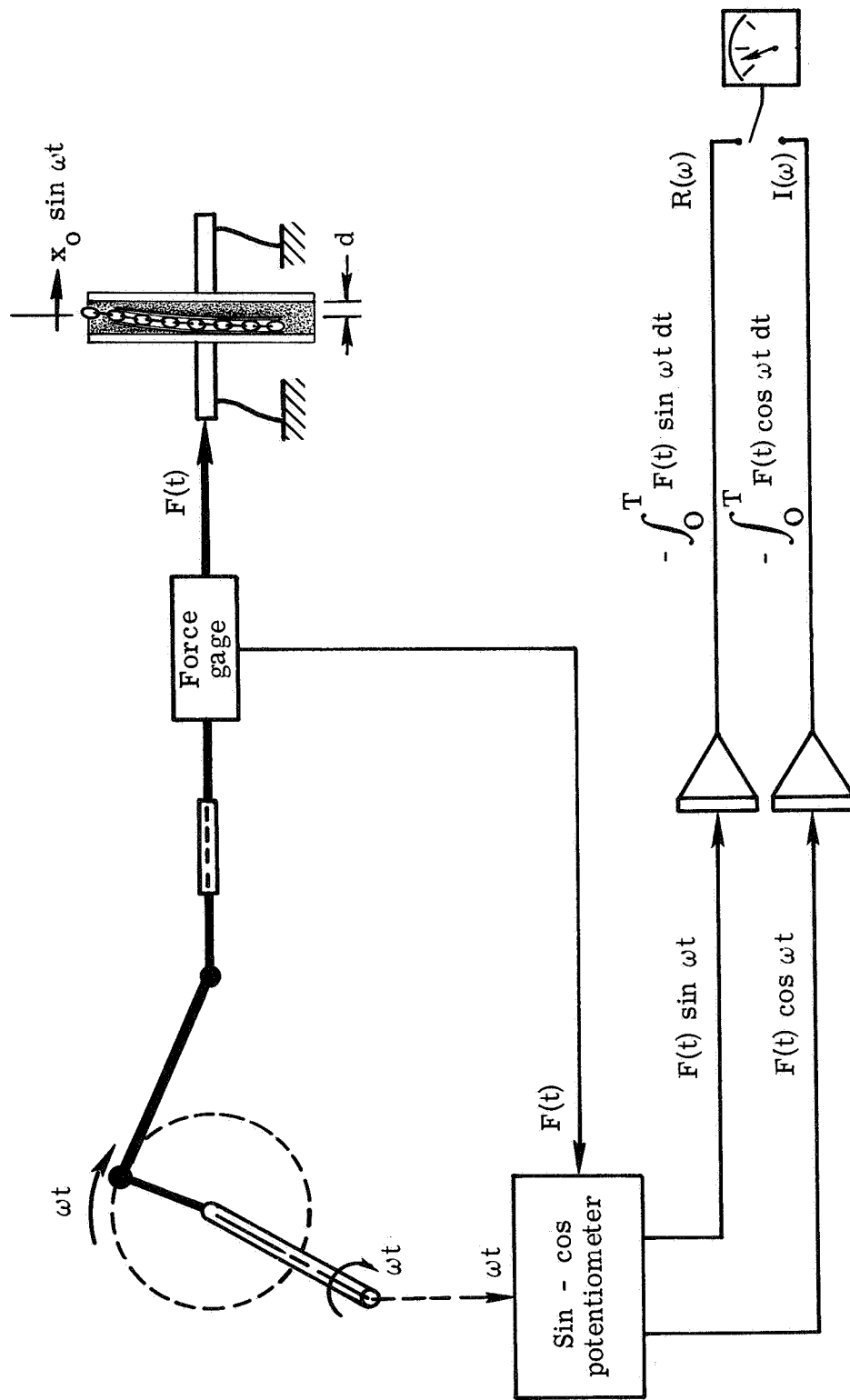


Figure 7.- Measurement of mechanical impedance of chain dampers.

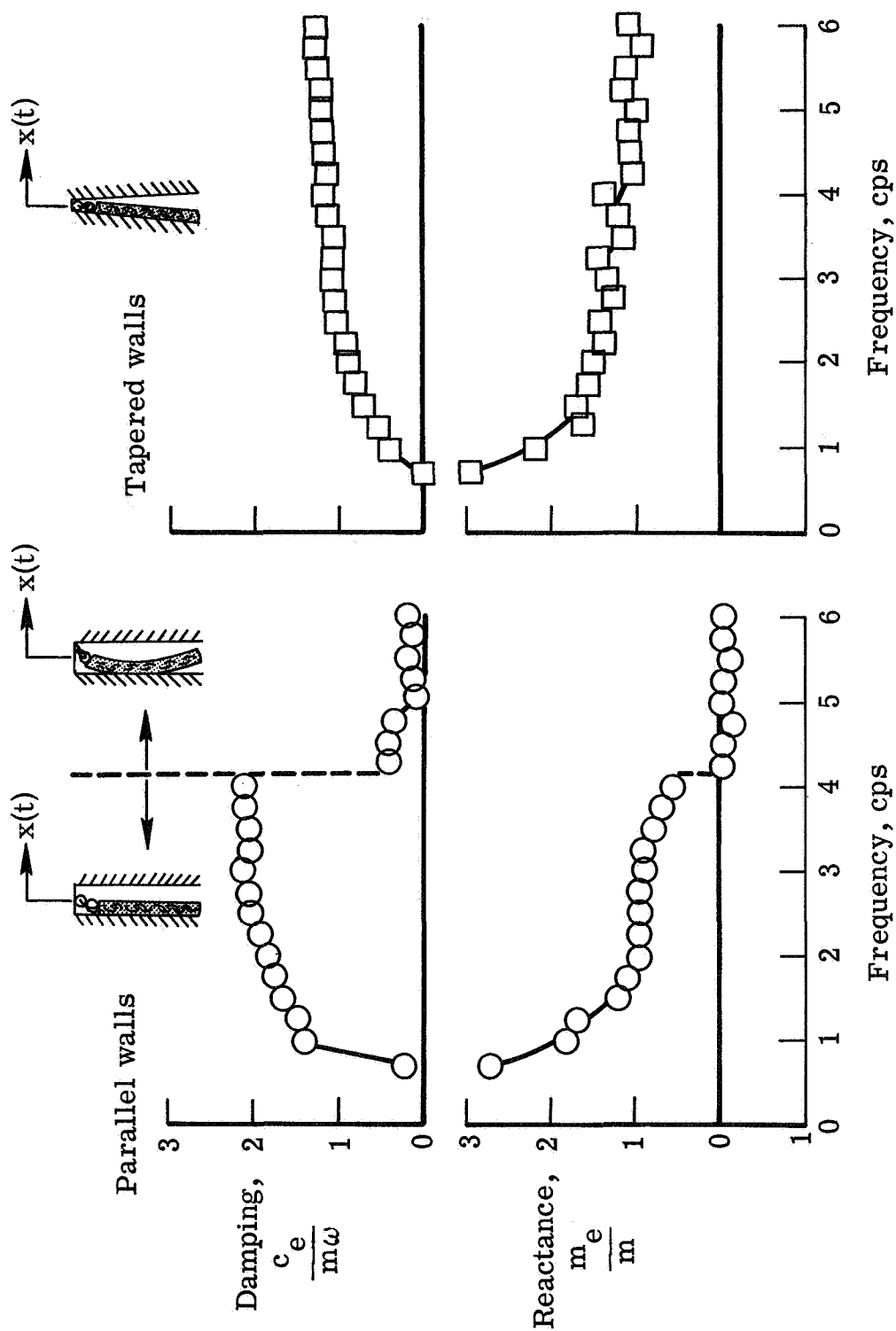


Figure 8.- Chain damper impedance measurements for parallel and tapered container walls.